Ni-doped MoS_2 Dry Film Lubricant Life

*Azhar Vellore Sergio Romero Garcia Nicholas Walters Duval Johnson Andrew Kennett Matthew Heverly Ashlie Martini**

A. Vellore, S. Romero Garcia, N. Walters, A. Martini

Mechanical Engineering Department

University of California Merced

5200 North Lake Rd

Merced, California 95343, USA

amartini@ucmerced.edu

D. A. Johnson, A. Kennett, M. Heverly

NASA Jet Propulsion Laboratory

4800 Oak Grove Dr, Pasadena, California 91109, USA

matthew.c.heverly@jpl.nasa.gov

Keywords: *MoS_2, doped MoS_2, dry film lubricant, wear, coating failure, 2D materials, solid lubricants*

The wear life of undoped and Ni-doped MoS_2 was evaluated at application-relevant pressure and speed conditions in air. It is found that the Ni-doped coatings outperformed the undoped coatings, particularly at lower pressure (faster speed) conditions. To understand this, the evolution of the coatings during run-in was characterized in terms of wear track depth, material composition and microstructure. It is found that wear depth exceeds the thickness of the coatings after hundreds of cycles, in sharp contrast to the wear life that was measured to be tens of thousands of cycles based on friction. This suggests that sliding was facilitated by MoS_2 continually worn from the sides of the wear track for most of the coating life. Further, microstructural analysis shows that the improved performance of Ni-doped coatings was attributable to cracking and delamination during the run-in stage, leading to more lubricious material available to facilitate sliding.

1 Introduction

Dry film lubricants (DFL) or solid lubricant coatings are preferred over liquid lubricants when operating conditions are extreme, e.g. very high or low temperature, vacuum or corrosive environments, or to prevent contamination of sensitive equipment [1, 2, 3]. Such conditions are present in various applications, but the prototypical example is space, where mechanical components must function

in extreme environments, including cryogenic temperature and vacuum. Liquid lubricants in space applications suffer from many issues, including volatility, condensation, degradation due to radiation and increase in viscosity at low temperatures [4, 5], resulting in reduced operating life, which is especially important for long duration missions. The alternative is DFLs, which are non-volatile and stable in extreme conditions. Perhaps the most widely used DFL for space applications is molybdenum disulfide (MoS_2). MoS_2 has a long history as a lubricant [6] and is currently used both in space and terrestrial applications as an additive in greases and lubricating oils, and as a DFL [7]. The lubricity of MoS_2 is provided by its crystal structure where stacked layers of MoS_2 basal planes (002) are held together by weak inter-planar van der Waals attraction which is easily overcome when the layers experience shear [8].

There are various techniques of fabricating MoS_2 dry films, including burnishing, sputtering, resin bonding and impingement. However, sputtered MoS_2 coatings are preferred for space applications [9] due to their tribologically superior performance in the absence of oxygen and humidity [10], good adhesion to substrates [11, 12] and absence of any binding agent that can outgas in vacuum conditions [13]. In a lab environment, the vacuum of space is often approximated by testing in dry nitrogen [14, 15, 16, 17, 18, 19, 20, 21]. Dry nitrogen simulates space vacuum conditions that are devoid of oxygen, water vapor and other elements that might affect the tribo-chemical processes occurring at the sliding interface [22]. Sputtered MoS_2 films exhibit excellent tribological performance in dry nitrogen with very low coefficient of friction (CoF) [23] and long wear life [15].

Despite the outstanding properties of sputtered MoS_2 coatings in environmental conditions devoid of oxygen and humidity, its tribological performance degrades significantly in ambient conditions [24, 25, 26, 27, 28, 29, 20]. This degradation is often attributed to oxidation resulting in MoO_3 and MoO_2 byproducts which impede the smooth sliding of MoS_2 basal planes. However, the topic is still a subject of debate and other mechanisms have been proposed, including water-restricted-growth of shear-induced highly ordered tribofilms [20, 30] and viscous friction due to water molecules between basal planes [31, 32]. Further, it was shown that water and oxygen in the atmosphere affected friction differently [16]. At room temperature, atmospheric oxygen had very little impact due to a low rate of oxidation, whereas physisorption and diffusion of water molecules increased friction. However, the opposite was observed at higher temperatures (>100 °C) where the thermal energy-driven oxidation rate exceeded the wear-driven surface oxide depletion rate, resulting in a net increase in oxidation

byproducts and higher friction, whereas water molecules desorbed readily and had little role to play [16].

The microstructure of sputtered MoS_2 is understood to play a significant role in its tribological behavior as well as its resistance to environmental conditions. Sputtered MoS_2 is known to have two possible morphologies, referred to as Types I and II, depending on the sputtering technique employed [33]. Type II consists of basal planes oriented parallel to the substrate resulting in dense packing and a low fraction of exposed edge sites. Type I morphology consists of basal planes oriented perpendicular to the substrate surface resulting in high porosity and exposed reactive edge sites. This Type I growth morphology is believed to have three distinct zones: starting from the substrate, there is a ridge structure, followed by a dense equiaxed zone, and finally a region of vertically oriented crystallites or columnar structures [34]. Most commercially produced MoS_2 DFLs are expected to exhibit Type I morphology due to the Direct Current (DC) sputtering technique used to produce them.

Many previous studies have characterized the friction and wear performance of Type I MoS_2. The Type I microstructure causes an oxidation-driven friction increase, beginning during the run-in period when the columnar crystallites are oriented perpendicular to the substrate, before being forced to reorient in the direction of sliding, trapping the oxidation byproducts between the crystallites and impeding shear [34, 35]. The friction after run-in depends on the rate of thermally driven formation of surface oxides and the rate of depletion of these oxides due to wear from the contact zone [16]. The wear behavior of Type I sputtered MoS_2 coating was studied by Spalvins [36] who showed that, at the onset of sliding, the vertical MoS_2 lamellae are first reoriented in the sliding direction and then later fracture at the base where they are attached to the equiaxed zone. Another study showed that basal plane reorientation occurs early in the sliding process, within 5% of the total wear life of the coating [13]. Based on this, it was proposed that the detached lamellae were depleted from the contact zone and subsequently did not contribute to the operational life of the coating. Lubrication after that point was therefore proposed to be provided by a thin ($\sim$200 nm) lubricating film remaining on substrate after the lamellae detached [36].

Co-depositing or doping certain metals with MoS_2 is known to affect the coating microstructure and can alleviate the detrimental effects of humidity and oxygen on the tribological behavior of sputtered coatings. Dopants are believed to improve the tribological properties of sputtered MoS_2

films through different mechanisms, including increased oxidation resistance [15, 37, 38] and increased hardness, [39, 40, 41, 42, 43, 44, 45] depending on the dopant material used. In an early study, Stupp [46] evaluated multiple transition metal dopants and found Cr, Co, Ni and Ta to be the best overall performers in terms of friction, wear life, ease of co-deposition and aging-related degradation.

Particularly for space applications, Ni is a preferred dopant [47] due to its ability to mitigate the increase of friction at low temperatures [48] and its low cost and availability [46]. In one study, [15] higher concentrations of Ni dopant (up to 20% by weight) were investigated and it was found that, above 11%, the coating becomes brittle and fails prematurely. For maximum coating life and stable friction, 5-7% Ni was recommended [46]. Co-depositing MoS_2 with Ni has been found to affect the morphology of the film as well. Specifically, pure MoS_2 and MoS_2 with 3% Ni showed Type I morphology, whereas doping with 9% or more Ni resulted in a "Zone T" microstructure which has a non-porous fibrous interior and flat tops [49]. However, how these changes in morphology due to Ni doping affect coating life is not known.

In summary, sputtered MoS_2 DFLs are preferred for space applications due to their excellent tribological performance in vacuum conditions devoid of oxygen and humidity. Sputtering results in MoS_2 microstructures that are believed to provide long life through processes that occur during run-in. Also, MoS_2 DFL performance, particularly friction at low temperatures, has been shown to improve with Ni doping. Although this improvement is attributed to the microstructure, the effect of Ni dopant on the morphological changes that occur during run-in is not understood. To address this, in the present study, we characterized the friction and wear behavior of sputtered doped and undoped MoS_2 films at different pressure and speed conditions. Long tests were run to determine coating life, as characterized by a drastic friction increase reflecting complete coating failure. Then, short tests were run to characterize and understand the run-in period during which it has been proposed that microstructural evolution occurs that plays a critical role in determining coating life. Results were analyzed in terms of both coating thickness, which is often assumed to correspond to life, and friction, reflecting actual useful life. Finally, findings were interpreted by analysis using microstructural and material characterization tools, including scanning electron microscopy (SEM) and energy dispersive spectroscopy (EDS).

2 Results and discussion

The microstructures of undoped and Ni-doped MoS_2 coating surfaces were characterized before tribological testing. The burnishing process applied after sputtering flattened the tops of the coatings, so images were taken at scratches on the burnished layer to reveal the microstructure of the material. The SEM micrographs in Figure 1 show that the undoped and Ni-doped coatings have similar microstructures, with highly columnar crystallites consistent with Type I coatings. The microstructures shown here are representative of images taken on multiple samples imaged at several different locations on the surface.

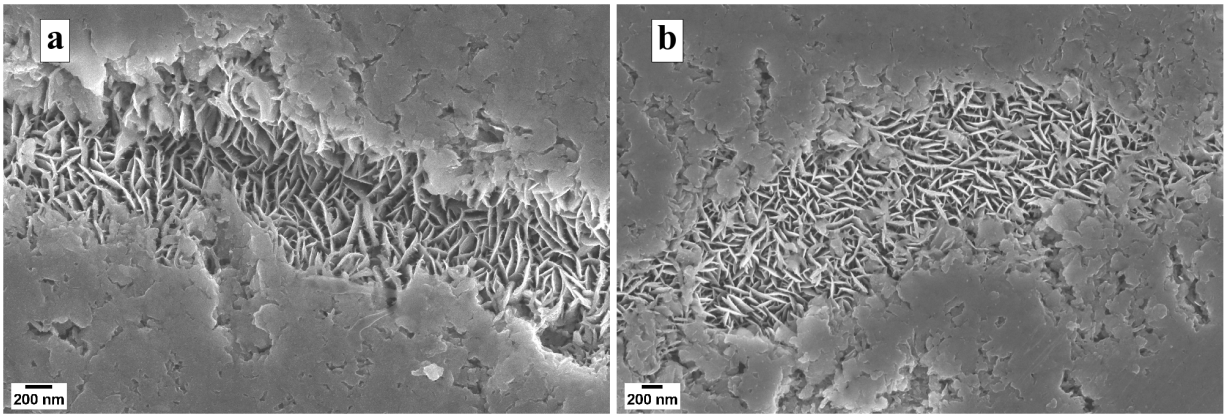

Figure 1: SEM micrographs of (a) undoped and (b) Ni-doped MoS_2 coating morphologies showing columnar structures consistent with Type I coatings and flat tops resulting from burnishing.

The performance of the undoped and doped MoS_2 coatings was measured at four different pressure/speed conditions. In the end-of-life tests, the CoF during sliding was tracked until the coating failed completely. Representative traces of the CoF as a function of number of cycles of rotation of the disk for undoped and Ni-doped coatings are shown in Figure 2. For these cases, the number of cycles until failure, i.e. wear life, is greater for the lower contact pressure / higher speed conditions. Also, the results indicate that Ni-doped coatings have longer life than the undoped coatings and that difference appears to be most significant at the lower contact pressures.

Coating failure was identified as the CoF exceeding and remaining above ≈ 0.4. We confirmed that the coating life identified using this criterion was reasonable by analysis of the elemental composition of unworn, partially worn and fully worn regions on the surfaces using EDS. The results for an undoped coating are shown in Figure 3. In this case there are two wear tracks shown: the track on the left corresponds to midway through a test (prior to failure) and the one on the right was taken at

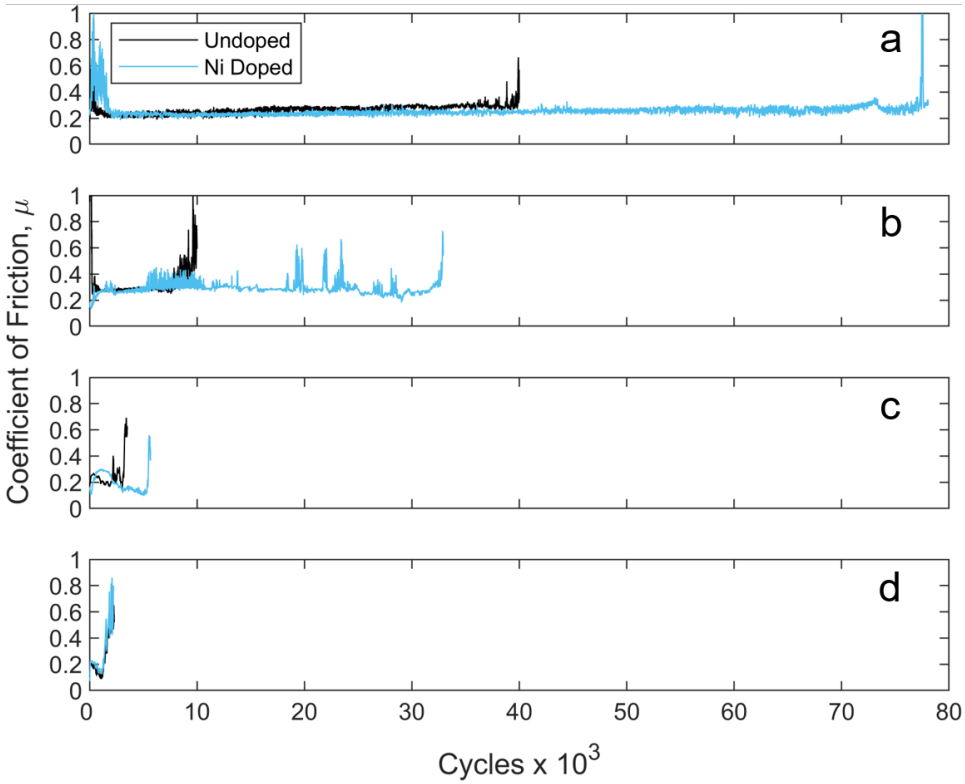

Figure 2: Representative CoF traces at (a) 300 MPa and 1 m/s (b) 500 MPa and 0.77 m/s (c) 800 MPa and 0.44 m/s, and (d) 1100 MPa at 0.1 m/s for undoped and Ni-doped MoS_2 coatings run until coating failure.

the end of a test (after failure). It is clear from the compositional maps of Molybdenum (Mo) and Sulfur (S) that the MoS_2 coating is fully worn on the right wear track with negligible Mo and S signal, while both Mo and S are observed on the left wear track obtained prior to failure. This is confirmed by observation of prominent Iron (Fe) and Chromium (Cr) signals from the steel substrate on the right wear track, after failure.

A similar EDS compositional map of unworn and full worn (after coating failure) regions of Ni-doped coating is shown in Figure 4. As expected, both fully worn tracks show negligible Mo and S signals, indicating the coating has been removed and prominent Fe and Cr signals from the steel substrate.

Wear life was measured from long duration tests at each pressure/speed condition for undoped and Ni-doped MoS_2 coatings. The results are shown in Figure 5, where the symbols represent the mean of three tests and the error bars reflect the standard deviation. The results indicate that Ni dopant improves the life of the MoS_2 coating at the lower contact pressures of 300 and 500 MPa, but the difference between doped and undoped coating life is not statistically significant at the higher contact pressures of at 800 and 1100 MPa. Also, the life of the Ni-doped coatings exhibits higher

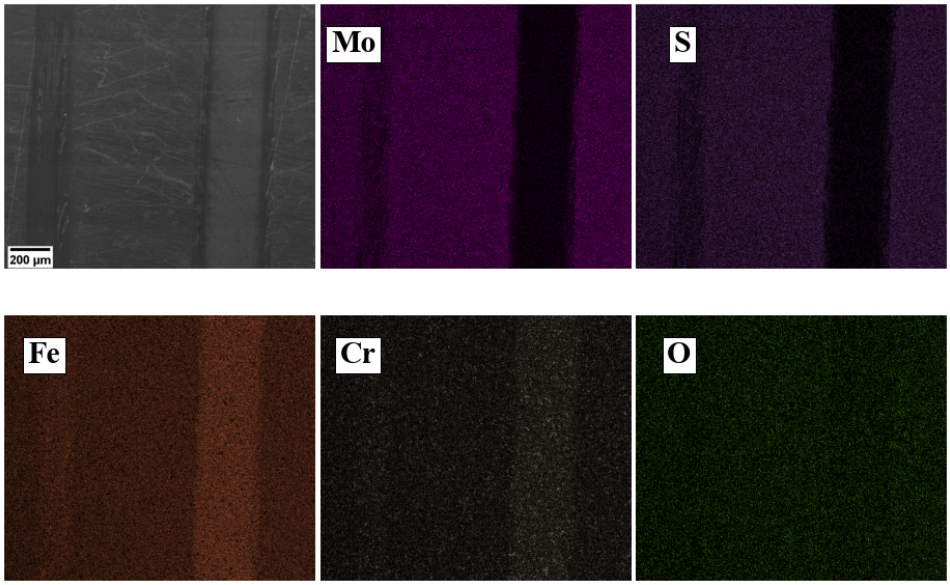

Figure 3: EDS compositional maps showing partially worn (left wear track), unworn (center region) and fully worn (right wear track) regions of undoped MoS_2 coating. The partial and fully worn tracks were generated in sliding tests at 300 MPa contact pressure after 18,000 and 80,000 cycles, respectively.

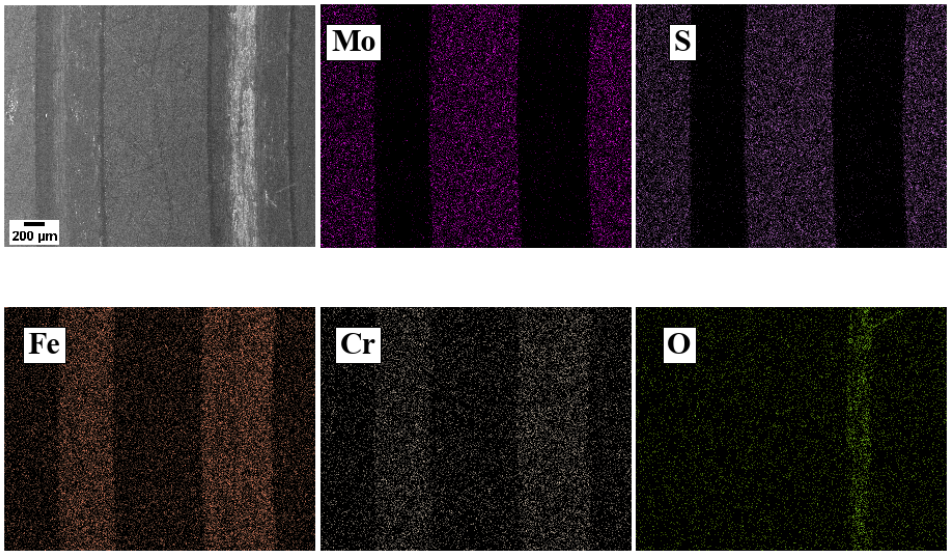

Figure 4: EDS compositional maps showing two fully worn wear tracks and unworn regions on a Ni-doped MoS_2 coating. The left and right tracks were generated in sliding tests at 500 MPa contact pressure after 34,000 and 43,000 cycles, respectively.

variability than the undoped coatings, particularly at the lower pressures. This may be attributed to non-uniformity in the distribution of Ni dopant in the coating on individual samples or from sample-to-sample, or greater variability in coating thickness for the doped samples.

Short duration tests were performed to study coating wear during run-in as a means of understanding wear mechanisms and how they are affected by the Ni dopant. For this, the rotating disk was stopped at different intervals of sliding and the 3D surface topography of the wear track at a fixed angular

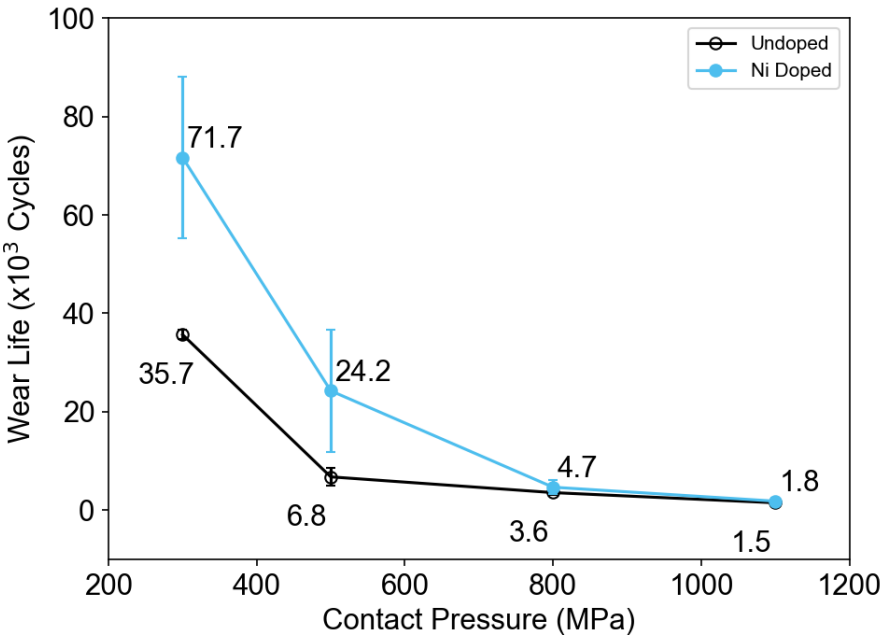

Figure 5: Wear life of undoped and Ni-doped MoS_2 at different contact pressure / sliding speed conditions. The results are plotted against pressure on the abscissa, but the speed is also different for each case. Ni dopant improves wear life compared to the undoped samples at low pressures.

position was measured using an interferometer. Then, the sliding was restarted from the location at which it was stopped. This technique enabled tracking of the evolution of the coatings during the wear process. In these tests, the coatings did not fail, as determined by the friction coefficient criterion used in the end-of-life tests. Representative cross-sections of the wear track obtained from the interferometer images at different number of cycles during run-in at the highest and lowest pressure are shown in Figure 6. These results indicate that wear depth generally increases with number of cycles and is greater for the higher pressure.

The wear depth was measured as the maximum depth of wear profiles such as those in Figure 6 from four tests on two different samples. The wear depth was then normalized by the coating thickness for each disk such that a normalized wear depth of 1 indicates that the coating has been completely removed. The average normalized wear depth is plotted as a function of number of cycles in Figure 7, where error bars represent the standard deviation. As expected, in all cases, the wear depth increases with number of cycles and is larger at the higher pressure. Also, notably, at either pressure, the wear tracks on the Ni-doped MoS_2 are shallower than those on the undoped MoS_2. This agrees qualitatively with the longer life of the Ni-doped coatings observed in the end-of-life tests at low pressure.

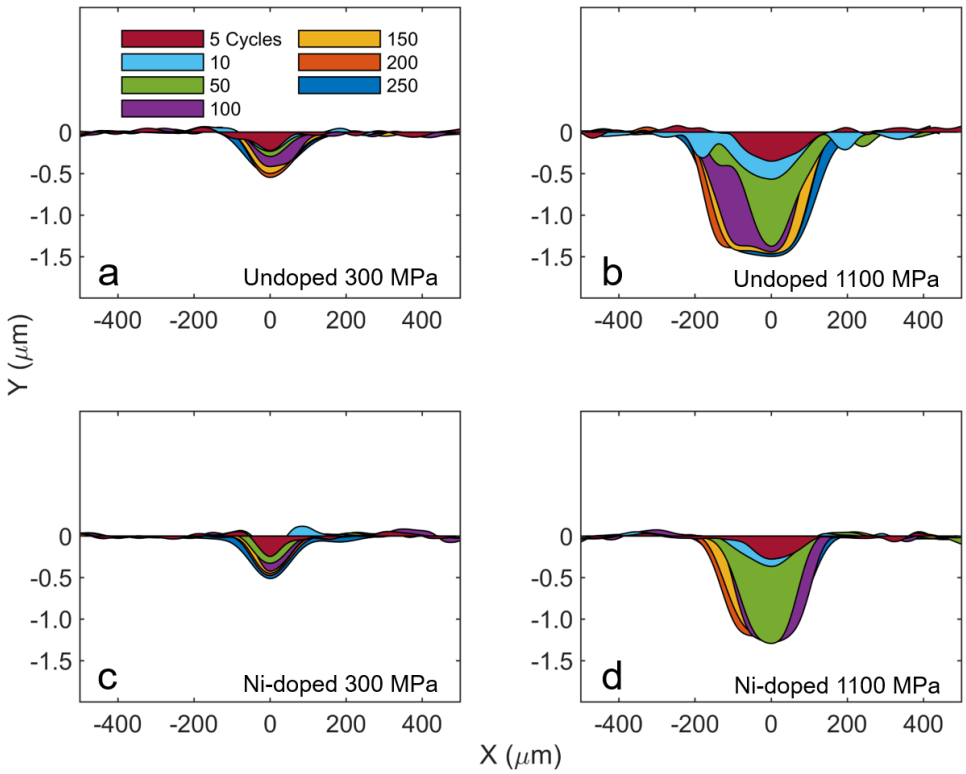

Figure 6: Wear profiles for (a) undoped MoS_2 at 300 MPa and 1 m/s, (b) undoped MoS_2 at 1100 MPa and 0.1 m/s, (c) Ni-doped MoS_2 at 300 MPa and 1 m/s, and (d) Ni-doped MoS_2 at 1100 MPa and 0.1 m/s showing the evolution of the wear tracks during the run-in tests.

Figure 7 also reveals different run-in behavior at low and high pressures. Specifically, the wear rate, i.e. rate of change of depth with cycles, is nearly constant throughout run-in at the low contact pressure. In contrast, at high pressure, the wear rate is initially very rapid but then decreases after about 100-150 cycles to a value similar to that observed at the low pressure. For the undoped coating at 1100 MPa, the normalized wear depth is unity (depth = coating thickness) after only 180 cycles. For the other cases, we used the rate of decrease of normalized wear depth with cycles after 150 cycles to estimate the number of cycles at which the normalized wear depth would reach unity. It was found that the wear depth would be equal to the coating thickness after 940±374 cycles for the undoped coating at low pressure and 1226±787 and 725±274 cycles for the Ni-doped coating at low and high pressure, respectively. This approximation assumes a linear wear rate, but we confirmed that the trend remained linear with additional tests to 1000 cycles on undoped coatings at high stress. Further, even if the rate becomes slightly sub-linear, these results predict that the wear depth would still exceed the coating thickness after hundreds of cycles, whereas the wear life was on the order of tens of thousands of cycles in Figure 5. This means that, for most of the life of the coating, very little of the "bulk" material is present in the wear track.

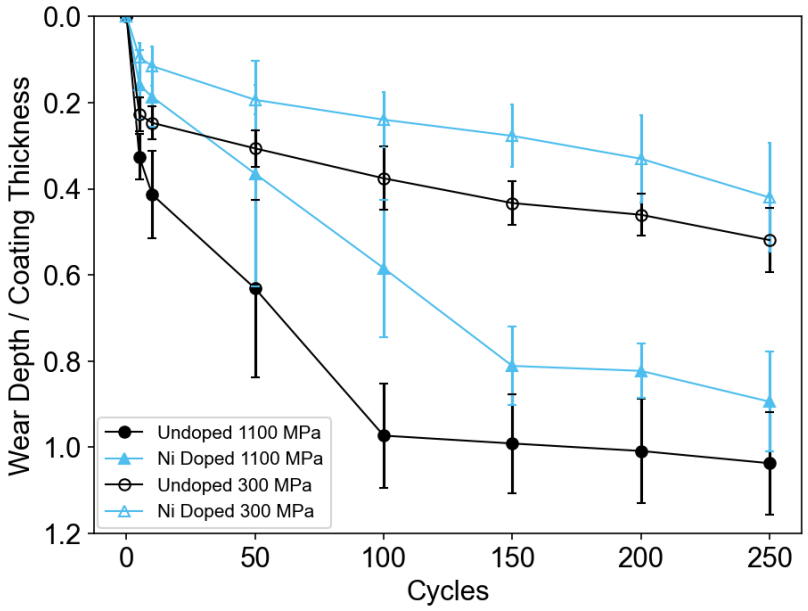

Figure 7: Wear depth as a function of cycle during run-in tests at 300 and 1100 MPa contact pressures on undoped and Ni-doped MoS_2. Wear tracks are shallower (less wear) on the Ni-doped sample at both pressures.

The implication of the above analysis is that the sliding contact is lubricated by local MoS_2 flakes or debris that form as the coating is worn. This was supported by the observation of MoS_2 on the ball observed via optical microscopy (not shown) after tens of thousands of cycles. We also characterized the coatings using SEM at the initial stages of run-in. Representative SEM micrographs of the wear tracks on the undoped and Ni-doped MoS_2 films after 10 cycles at 1100 MPa and 0.1 m/s are shown in Figure 8. On both the doped and undoped samples, we observe significant wear, even after only 10 cycles. However, the wear mechanism appears to differ between doped and undoped. Specifically, while both coatings exhibit cracking, there is also delamination in the case of the Ni-doped sample (Figure 8b) that is not observed on the undoped sample (Figure 8a). Based on the microstructure of these Type I coatings, it is presumed that the columnar zone is cracking and/or delaminating. This difference in failure mode has also been reported in a previous study where sputtered MoS_2 with 9% Ni exhibited more delamination in indentation tests than pure or low Ni concentration MoS_2 [50].

It has been suggested that the columnar zone of Type I MoS_2 sits on a lower layer of material, called the equiaxed zone [34]. SEM images of the regions between the cracks on the doped and undoped coatings after 10 cycles are shown in Figure 9. These examples, that are representative of images taken at various locations on the worn surfaces, exhibit clear differences between the coatings. Notably, the material under the cracked or delaminated columnar zone for the undoped coating is

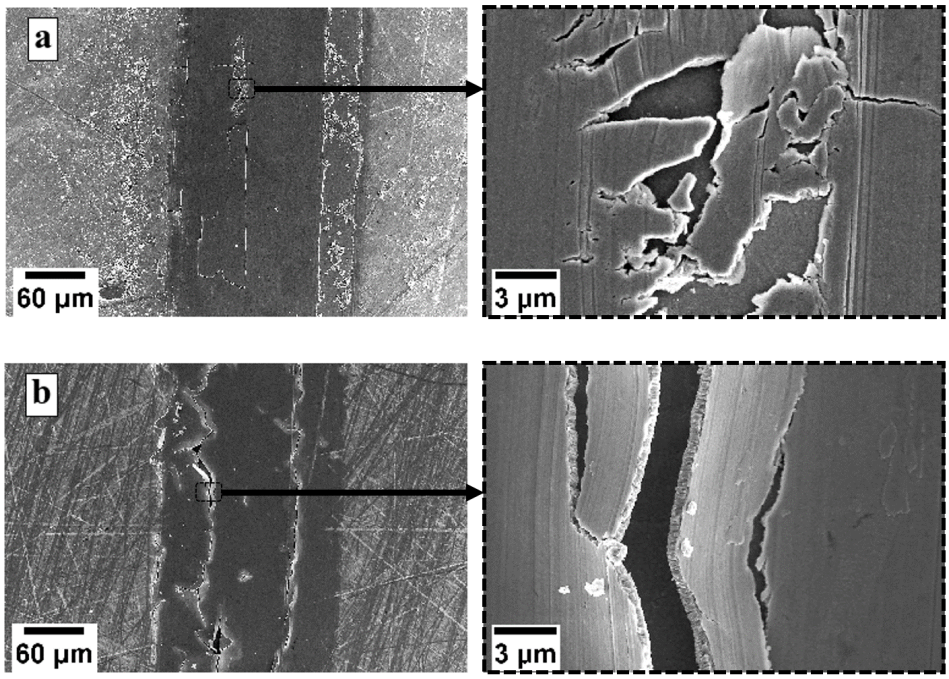

Figure 8: SEM micrographs of (a) undoped and (b) doped MoS_2 coatings after 10 cycles at 1100 MPa and 0.1 m/s. The images on the right show close-up views of the partially worn material. These images show representative features where the undoped coatings exhibit cracking while the doped coatings exhibit cracking and delamination.

smooth while that for the Ni-doped coating is rough. This may be attributable to differences in the microstructure of the doped coating that arise during sputtering. Alternatively, it could be related to the delamination that was observed only for Ni-doped coatings and may have occurred through breaking of columnar structure, leaving partial columns on the surface.

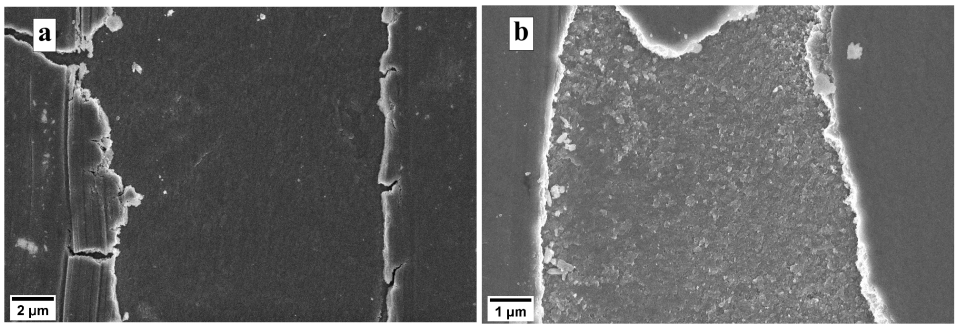

Figure 9: SEM micrographs of the regions between the cracked or delaminated columnar zone for (a) undoped and (b) Ni-doped MoS_2 coating after 10 cycles at 1100 MPa and 0.1 m/s. The material underneath the failed columnar zone is distinctly rougher for the Ni-doped coating.

The fact that the wear depth appeared to exceed the coating thickness after very few cycles (compared to the wear life) suggested the contact was lubricated by localized MoS_2 flakes or debris. Based on the images in Figure 8 these flakes could have formed through cracking or delamination of the columnar zone. Representative images of some of flakes from tests run to 10 or 250 cycles

are shown in Figure 10. First, in all cases, the thickness of the flakes (as approximated from these images) is on the order of a few hundred nanometers. This is less than the expected coating thickness, suggesting that the columnar zone gets denser due to the contact pressure. Also, the flakes at 10 cycles (Figures 10a and b) appear to retain more of the original columnar structure (Figure 1) than the flakes imaged at 250 cycles (Figures 10c and 10d). This difference may be attributable to crystalline reorientation suggested in previous studies [34, 35, 13]. However, there is no obvious difference between the cross-sections of the flakes from the undoped (Figure 10c) and Ni-doped (Figure 10d) coatings.

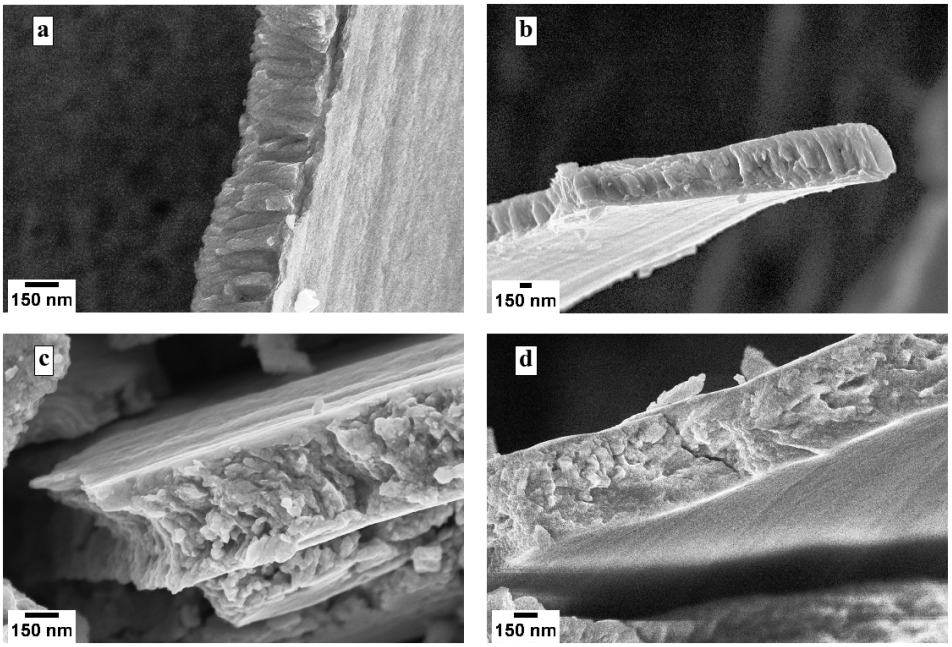

Figure 10: SEM micrographs of dense flakes of MoS_2 within or near the wear track from run-in tests of (a and b) Ni-doped coatings after 10 cycles, (c) an undoped coating after 250 cycles, and (d) a Ni-doped coating after 250 cycles. All images from tests at 1100 MPa and 0.1 m/s.

The SEM evidence supports the hypothesis that most of the life of the coating is provided by flakes of material. However, these flakes must be supplied continuously throughout the life of the coating. Since the depth of the wear track exceeds the coating thickness at the high pressure, the flakes cannot be coming from the bottom of the wear track. Rather, it is likely that they are replenished from the sides of the wear track, i.e. as the width of the worn region increases, additional cracking and/or delamination provides newly available lubricious material. We tested this hypothesis by measuring the wear track width (full width at half maximum) during the run-in tests. The results shown in Figure 11 indicate that wear width increases with cycles, but at a much slower rate than the wear

depth in Figure 7. Note that, although the wear width appears to plateau after a few hundred cycles at 300 MPa, in fact the width continues to increase throughout the test (e.g. the widths of the wear tracks in the EDS images in Figure 3 are several times larger than the apparent plateau in Figure 11). Generally, the observation of increasing wear width is consistent with the hypothesis that worn material is gradually removed from the sides of the wear track to lubricate the contact.

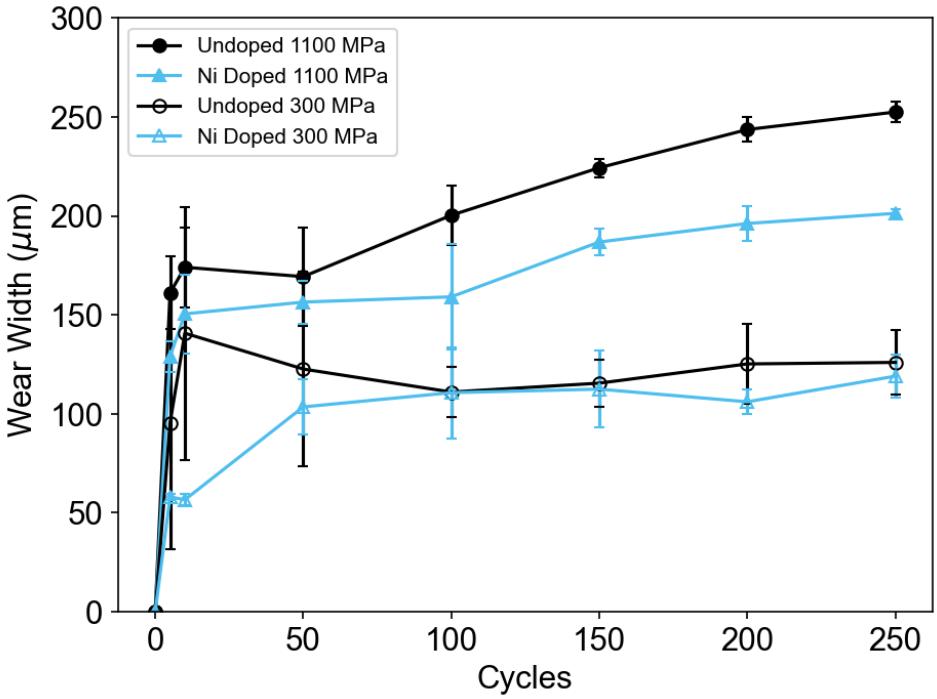

Figure 11: Wear width as a function of cycle during run-in tests at 300 and 1100 MPa contact pressures on undoped and Ni-doped MoS_2. Wear tracks widths are larger at the higher pressures. In all cases, the width increases gradually with sliding cycles.

All of the above suggests a mechanism by which MoS_2 coatings provide low friction and wear by generating flakes of lubricious material at the edges of the wear track. The remaining question is why Ni-doped coatings wear more slowly during run-in and have longer wear life at low pressures. One explanation is the Ni-doped coatings are harder, since increased hardness is one mechanism by which dopants have been proposed to improve the tribological performance of MoS_2 [46, 15]. However, the different failures modes observed in Figure 8 as well as the differences in the material underneath the cracked/delaminated columnar zone in Figure 9 suggest there may be another contributing factor. The observation that coating performance is enabled by flakes of worn material suggests that the Ni-doped coating generates more lubricious and/or longer-lasting flakes. Specifically, it is likely that delamination yields more and potentially larger and denser flakes of columnar material than cracking.

To investigate this hypothesis, we performed progressive load scratch testing following the ASTM C1624-05 standard. This test involves scratching the surface using a sphero-conical diamond indenter of radius 200 μm at normal load progressively increased from 5 to 80 N at a sliding speed of 10 mm/min. The lateral force on the indenter was recorded and plotted against time as shown in Figure 12(a). There is no abrupt change in the lateral force during any of these tests, indicating that either there was no 'damage event' due to coating failure or the coating failed at the onset of sliding. Also, the lateral force on the Ni-doped coating is slightly (although statistically significantly) lower than that on the undoped coating.

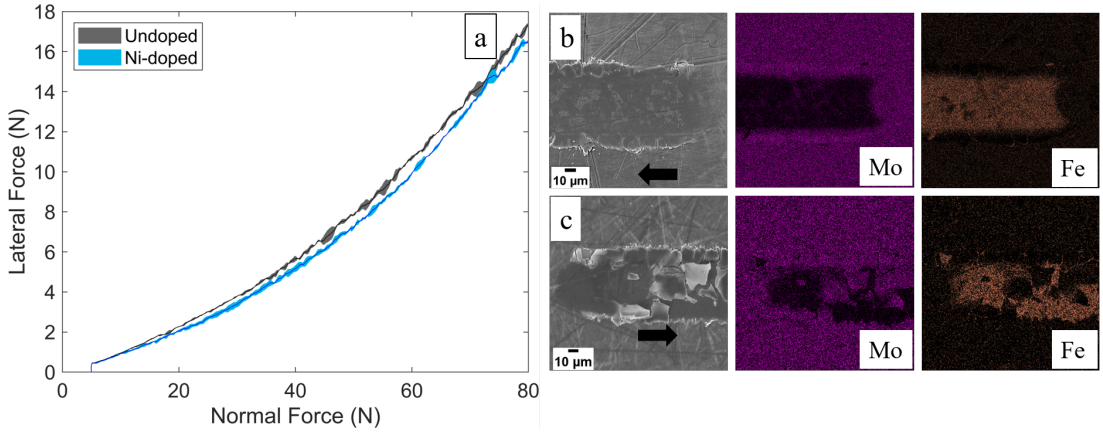

Figure 12: (a) Average lateral force during progressive load scratch tests on doped and undoped samples. Lines represent the average of three tests and the band represents standard deviation. SEM images and Mo/Fe signals from EDS taken at the start of the test on (b) undoped and (c) Ni-doped coatings.

This difference was investigated using SEM and EDS of the scratched region . Representative images taken from the beginning of the scratch (around 5 N load) are shown in Figure 12(b) and (c). From the SEM images, the difference in the wear modes of these coatings is apparent: the undoped coating is almost fully worn in the contact zone, whereas Ni-doped coating is still partly intact with some signs of delamination. This was confirmed by the elemental composition maps that show Mo remains in the scratched region only in the case of the Ni-doped coating; similarly, the Fe signal is much stronger for the undoped coating.

SEM images take later in the test at higher loads (about 62 N) are shown in Figure 13. These results confirm both the coatings are fully worn. In the middle of the wear track, both surfaces have semi-circular features oriented in the sliding direction that are the result of conformal accumulation of plastically-deformed substrate material. However, the two surfaces differ at the edge of the wear track where there is more spallation and delamination for the Ni-doped coating. This corroborates

the hypothesis that the Ni-doped coating generates more material from the sides of the wear track.

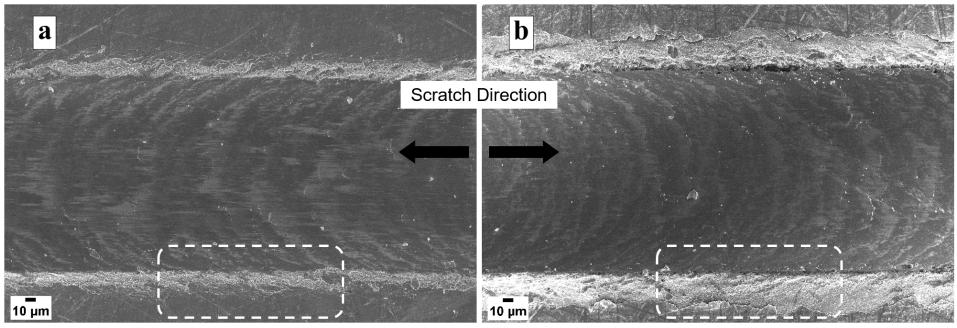

Figure 13: SEM micrographs of (a) undoped and (b) Ni-doped MoS_2 coatings during a representative progressive load scratch test (at approximately 62 N load). The doped and undoped coatings are distinctly different at the edges of the wear tracks (for example, the regions identified by the dashed lines).

The evidence presented strongly suggests that the Ni-doped MoS_2 coatings have longer wear life because of their ability to generate more lubricious material from the sides of wear track. This mechanism is likely complemented by increased hardness, as observed for doped MoS_2 coatings in previous studies. The complete proposed mechanism is illustrated in Figure 14. The columnar zone is compressed in the first few cycles and then begins cracking (undoped) or delaminating (Ni-doped), leading to the formation of lubricious flakes. Although the coating is worn through in the center of the wear track, the track width gradually increases with cycles, resupplying lubricating flakes to the contact over the remaining life of the coating.

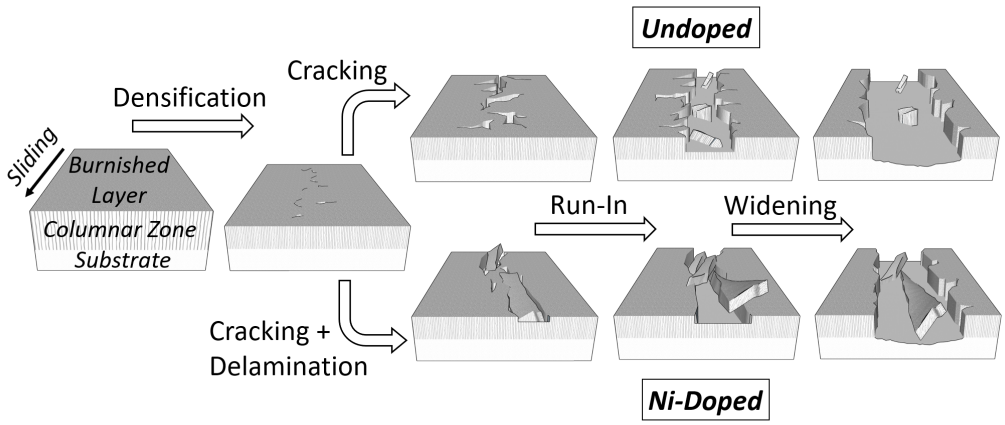

Figure 14: Schematic illustration of the proposed wear process that occurs through densification followed by cracking and, for Ni-doped MoS_2, delamination. The flakes generated during the cracking and/or delamination process lubricate the contact subsequently as they are continuously supplied as the wear track widens and more flakes are made available to facilitate sliding.

3 Conclusion

In this study, the effect of Ni dopant on wear life and morphological evolution of sputtered MoS_2 coatings was investigated. Tribological experiments at different pressure and speed conditions were performed to measure and compare the wear life of Ni-doped and undoped MoS_2 coatings. The results showed that Ni dopant at $\approx 7\%$ by wt. concentration improved wear life of MoS_2 coatings significantly at low contact pressures. However, Ni-doped coatings exhibited higher variability in wear life than undoped coatings, possibly due to non-uniformity in Ni distribution or coating thickness in doped samples.

Similar tests were performed for short duration (5 to 250 cycles) at low and high pressure conditions to study the evolution of wear during run-in. This process was characterized in terms of wear depth, wear width and coating microstructure. At both low and high pressure conditions, the wear depth either exceeded or was expected to exceed (based on extrapolation of the wear rate) the coating thickness early in the run-in process, suggesting that very little of the "bulk" material was left in the wear track for most of the life of the coating. This result implied that the contact was being lubricated by detached MoS_2 debris or flakes, which was supported by SEM micrographs showing cracked and/or delaminated coating in the wear track after the first 10 cycles. The gradual increase of wear width of the coating suggested that lubricious flakes of MoS_2 were supplied to the contact from the sides of the wear track as the width of the worn region increased.

SEM imaging suggested that the undoped and Ni-doped coatings exhibited different wear mechanisms, with the former wearing by cracking while the latter demonstrated cracking and delamination. Analysis of progressive load scratch tests confirmed that wear behavior differed between the doped and undoped coatings, particularly at the edges of the worn regions. The delamination exhibited by the Ni-doped coatings may explain its longer wear life since delamination yields more and possibly larger and denser flakes than those generated by cracking of undoped coatings.

More generally, the findings of this study illustrate that the wear life of MoS_2 coatings cannot be correlated to wear track depth, in contrast to the usual concept of wear for traditional engineering materials. Further, the results suggest a new mechanism by which dopants can extend MoS_2 dry film lubricant life, i.e. facilitating delamination, that might be leveraged to further understand and then improve the performance of these materials.

4 Experimental Section

4.1 Materials

Two coatings were investigated in this study: undoped MoS_2 and $\approx 7\%$ wt Ni-doped MoS_2. Both types of coatings were fabricated via DC sputter deposition with electron beam assist. Stainless steel (440C) disks of 0.25" thickness, hardness 45-50 HRC or 58-62 HRC with average surface roughness of 80 nm were used as substrates. The coating thickness varied slightly from disk to disk, but was in the range of 0.8 to 2.0 μm for all disks. A burnishing process was applied to the coated disks to obtain a smooth reflective surface finish. Burnishing involved sliding a wool-like material against the sputtered disks until coated surface had a uniform appearance and there was no more loose debris coming off the surface onto the wool.

4.2 Test Conditions

Tribological testing to measure friction and wear was performed using an Rtec Instruments tribometer and white light interferometer. Unidirectional sliding tests using a ball-on-disk set-up as described by the ASTM G-99 standard were performed to measure CoF. 440C stainless steel balls with Rockwell C60 hardness were used as the counterbody. The radius of the circular sliding path on the disks was between 15 and 30 mm All test were carried out at room temperature and ambient air conditions with relative humidity ranging between 30–50%.

Table 1 shows the load and speeds used in the testing and the calculated maximum Hertz contact pressures. Note that the sliding speed was also varied to simulate the inverse stress (analogous to torque) and speed relationship typical in a gear-driven system. Two types of sliding tests were performed in this work, end-of-life and run-in. End-of-life tests were used to determine the wear life in terms of number of revolutions/cycles to failure. This test involved sliding on the coated disk until the CoF increased above ≈ 0.4, became characteristically noisy and did not drop back to lower values. Run-in tests were short duration sliding tests (between 5 and 250 cycles) used to study the evolution of wear and wear mechanisms. Only 300 MPa and 1100 MPa contact pressures were studied for run-in. Another distinction between the end-of-life and run-in tests is that, in the former, the disk was already rotating before the ball was pressed against it whereas in the latter, the disk was rotated after loading. Three repeat end-of-life tests and four repeat run-in tests were performed per case.

Table 1: Experimental parameters used in the ball-on-disk tests. High pressures are matched with low speed, and vice versa, to mimic the operating conditions of a gearing system.

Normal Load (N)	Contact Pressure (MPa)	Sliding Speed (m/s)
0.27	300	1
2.5	500	0.77
5.1	800	0.44
13.3	1100	0.1

4.3 Analysis

3D surface images of the wear tracks were obtained using a white light interferometer. The interferometer was calibrated to be within 1% of reference values. Wear depth was measured from 2D profiles taken at different positions on the wear track using the image processing software Gwyddion. The mean wear depth at four angular positions on each wear track was calculated and reported with error bars representing the standard deviation from the mean. Energy Dispersive Spectroscopy (EDS) using EDAX Genesis spectrometer attached to a FEI Quanta 200 Environmental scanning electron microscope (SEM) was used to obtain elemental composition in wear tracks. The microstructure of the coating before and after sliding was characterized using a Zeiss Gemini 500 SEM.

Acknowledgements

Research at UC Merced was partially supported by the Merced nAnomaterials Center for Energy and Sensing (MACES) through the support of the National Aeronautics and Space Administration (NASA) grant no. NNX15AQ01. A portion of this research was carried out at the Jet Propulsion Laboratory, California Institute of Technology and was sponsored by NASA (80NM0018D0004). A portion of this work was funded by the Historically Black Colleges and Universities/Minority Serving Institutions (HBCU/MSI) program run by the Engineering and Science Directorate at JPL. Reference herein to any specific commercial product, process, or service by trade name, trademark, manufacturer, or otherwise, does not constitute or imply its endorsement by the United States Government or the Jet Propulsion Laboratory, California Institute of Technology.

References

[1] J. R. Lince, In P. L. Conley, editor, *Space Vehicle Mechanisms: Elements of Successful Design*, 153. John Wiley & Sons, **1998**.

[2] C. Donnet, A. Erdemir, *Surf. Coat. Tech.* **2004**, *180* 76.

[3] X. Sun, *Solid Lubricants for Space Mechanisms*, Springer US, Boston, MA, ISBN 978-0-387-92897-5, **2013**.

[4] M. J. Jansen, W. R. Jones, S. V. Pepper, *Tribol. Lett.* **2003**, *14*, 2 61.

[5] R. L. Fusaro, M. M. Khonsari, *NASA Technical Report* **1992**, , 105198.

[6] D. H. Killeffer, A. Linz, *Molybdenum Compounds, Their Chemistry and Technology*, Interscience Publishers, **1952**.

[7] M. R. Vazirisereshk, A. Martini, D. A. Strubbe, M. Z. Baykara, *Lubricants* **2019**, *7*, 7 57.

[8] I. Song, C. Park, H. C. Choi, *RSC Adv.* **2015**, *5*, 10 7495.

[9] In P. L. Conley, editor, *Space Vehicle Mechanisms: Elements of Successful Design*. John Wiley & Sons, **1998**.

[10] E. W. Roberts, *Thin Solid Films* **1989**, *181*, 1-2 461.

[11] P. D. Fleischauer, *Thin Solid Films* **1987**, *154*, 1-2 309.

[12] E. W. Roberts, *NASA. Lewis Research Center 20th Aerospace Mechanics Symposium* **1986**, 103–119.

[13] M. R. Hilton, R. Bauer, P. D. Fleischauer, *Thin Solid Films* **1990**, *188*, 2 219.

[14] H. Li, T. Xu, C. Wang, J. Chen, H. Zhou, H. Liu, *J. Phys. D: Appl. Phys.* **2004**, *38*, 1 62.

[15] J. S. Zabinski, M. S. Donley, S. D. Walck, T. R. Schneider, N. T. McDevitt, *Tribol. Trans.* **1995**, *38*, 4 894.

[16] H. S. Khare, D. L. Burris, *Tribol. Lett.* **2013**, *52*, 3 485.

[17] A. A. Voevodin, J. P. O'Neill, J. S. Zabinski, *Surf. Coat. Tech.* **1999**, *116* 36.

[18] A. A. Voevodin, T. A. Fitz, J. J. Hu, J. S. Zabinski, *J. Vac. Sci. Technol. A* **2002**, *20*, 4 1434.

[19] A. A. Voevodin, J. S. Zabinski, *Compos. Sci. Technol.* **2005**, *65*, 5 741.

[20] J. F. Curry, N. Argibay, T. Babuska, B. Nation, A. Martini, N. C. Strandwitz, M. T. Dugger, B. A. Krick, *Tribol. Lett.* **2016**, *64* 11.

[21] P. Serles, H. Sun, G. Colas, J. Tam, E. Nicholson, G. Wang, J. Howe, A. Saulot, C. V. Singh, T. Filleter, *Advanced Materials Interfaces* **2020**, 1901870.

[22] P. J. John, J. N. Cutler, J. H. Sanders, *Tribol. Lett.* **2001**, *9*, 3-4 167.

[23] C. Donnet, J. M. Martin, T. Le Mogne, M. Belin, *Tribol. Int.* **1996**, *29*, 2 123.

[24] M. Tagawa, J. Ikeda, H. Kinoshita, M. Umeno, N. Ohmae, In T. R. Kleiman, J., editor, *Protection of Space Materials from the Space Environment*, 73–84. **2001**.

[25] T. Liang, W. G. Sawyer, S. S. Perry, S. B. Sinnott, S. R. Phillpot, *J. Phys. Chem. C* **2011**, *115*, 21 10606.

[26] S. Ross, A. Sussman, *J. Phys. Chem.* **1955**, *59*, 9 889.

[27] A. J. Haltner, C. S. Oliver, *Ind. Eng. Chem. Fund.* **1966**, *5*, 3 348.

[28] R. P. Pardee, *ASLE Trans.* **1972**, *15*, 2 130.

[29] J. K. G. Panitz, L. E. Pope, J. E. Lyons, D. J. Staley, *J. Vac. Sci. Technol. A* **1988**, *6*, 3 1166.

[30] J. F. Curry, M. A. Wilson, H. S. Luftman, N. C. Strandwitz, N. Argibay, M. Chandross, M. A. Sidebottom, B. A. Krick, *ACS Appl. Mater. Inter.* **2017**, *9*, 33 28019.

[31] M. Uemura, K. Saito, K. Nakao, *Tribol. Trans.* **1990**, *33*, 4 551.

[32] G. Levita, M. C. Righi, *Chem. Phys. Chem* **2017**, *18*, 11 1475.

[33] J. Haider, *MoSx Coatings by Closed-Field Magnetron Sputtering*, 2323–2333, Springer US, Boston, MA, ISBN 978-0-387-92897-5, **2013**.

[34] T. Spalvins, *Thin Solid Films* **1982**, *96*, 1 17.

[35] V. Buck, *Wear* **1983**, *91*, 3 281.

[36] T. Spalvins, *J. Vac. Sci. Technol. A* **1987**, *5*, 2 212.

[37] M. C. Simmonds, A. Savan, E. Pflüger, H. Van Swygenhoven, *Surf. Coat. Tech.* **2000**, *126*, 1 15.

[38] J. J. Nainaparampil, A. R. Phani, J. E. Krzanowski, J. S. Zabinski, *Surf. Coat. Tech.* **2004**, *187*, 2-3 326.

[39] N. M. Renevier, V. C. Fox, D. G. Teer, J. Hampshire, *Surf. Coat. Tech.* **2000**, *127*, 1 24.

[40] D. G. Teer, *Wear* **2001**, *251*, 1-12 1068.

[41] A. A. Tedstone, D. J. Lewis, P. O'Brien, *Chem. Mater.* **2016**, *28*, 7 1965.

[42] M. Ye, G. Zhang, Y. Ba, T. Wang, X. Wang, Z. Liu, *Appl. Surf. Sci.* **2016**, *367* 140.

[43] P. Stoyanov, R. R. Chromik, D. Goldbaum, J. R. Lince, X. Zhang, *Tribol. Lett.* **2010**, *40*, 1 199.

[44] A. Paul, H. Singh, K. C. Mutyala, G. L. Doll, In *44th Aerospace Mechanisms Symposium.* **2018** 141.

[45] H. Li, X. Li, G. Zhang, L. Wang, G. Wu, *Tribol. Lett.* **2017**, *65*, 2 38.

[46] B. C. Stupp, *Thin Solid Films* **1981**, *84*, 3 257.

[47] J. R. Lince, *Doped MoS_2 Coatings and Their Tribology*, 782–785, Springer US, Boston, MA, ISBN 978-0-387-92897-5, **2013**.

[48] M. A. Hamilton, L. A. Alvarez, N. A. Mauntler, N. Argibay, R. Colbert, D. L. Burris, C. Muratore, A. A. Voevodin, S. S. Perry, W. G. Sawyer, *Tribol. Lett.* **2008**, *32*, 2 91.

[49] M. R. Hilton, G. Jayaram, L. D. Marks, *J. Mater. Res.* **1998**, *13*, 4 1022.

[50] M. R. Hilton, *Surf. Coat. Tech.* **1994**, *68* 407.

5 Table of Contents

Ni doping improves the wear life of MoS_2 dry film lubricants. Wear depth exceeds coating thickness after hundreds of sliding cycles, a fraction of the total coating life. Results suggest sliding facilitated by MoS_2 continually worn from the sides of the wear track, and the improved performance of Ni-doped coatings is attributed to cracking and delamination producing more lubricious material.

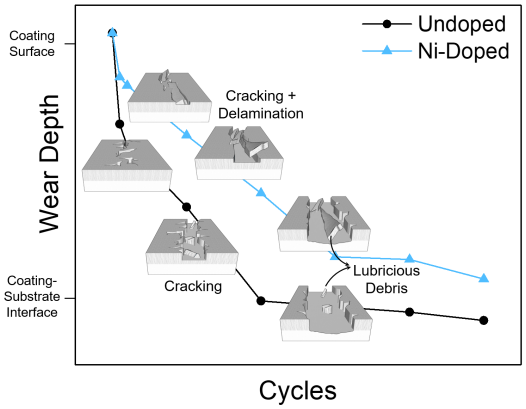
Undoped
Ni-Doped
Coating Surface
Wear Depth
Cracking + Delamination
Cracking
Lubricious Debris
Coating-Substrate Interface
Cycles